Infrared Emission and Theoretical Study of Carbon Monoxide Adsorbed on Alumina-Supported Rh, Ir, and Pt Catalysts

Tamás I. Korányi,*,† Judith Mihály,† Éva Pfeifer,† Csaba Németh,† Tatiana Yuzhakova,‡ and János Mink†,‡

Department of Molecular Spectroscopy, Institute of Structural Chemistry, Chemical Research Center of the Hungarian Academy of Sciences, P. O. Box 17, H-1525 Budapest, Hungary, and Analytical Chemistry Research Group, Hungarian Academy of Sciences and Faculty of Informatical Technology, Research Institute of Chemical and Process Engineering, University of Veszprém, H-8200 Veszprém, Hungary

Received: October 9, 2005; In Final Form: November 24, 2005

The infrared emission spectra of CO adsorbed on alumina-supported 1, 3, and 5 wt % Rh, Ir, and Pt metal-containing catalysts were studied at 423 and 473 K. While CO is adsorbed in dicarbonyl (dimer), linearly (on-top) bonded and bridged carbonyl forms on rhodium and platinum, the dimer form is dominant on iridium. The relative intensity of Rh−CO and Ir−CO linear bands decrease with increasing temperature compared to the intensity of the dicarbonyl bands; the corresponding bands on Pt behave the opposite way. Two dicarbonyl and two linear Pt−CO bands were identified in the infrared spectra of Pt/Al_2O_3 catalysts. The surface structure (kinked or planar Pt atoms), the dispersity of the metal, the temperature, and the quantity of adsorbed CO on the surfaces all have an effect on the fine structure of the Pt−CO stretching bands. The metal−carbon and CO stretching force constants were calculated for surface dicarbonyl, linearly bonded CO, and bridged carbonyl species. The metal−carbon stretching wavenumbers and force constants were predicted and compared between surface species and metal carbonyl complexes. The iridium−carbon bonds were found always stronger than the Rh−C and Pt−C ones in all surface species. The observed stretching wavenumbers and force constants seem to support the idea that CO and metal−carbon bonds are always stronger in metal carbonyl complexes than in adsorbed surface species. The distribution and mode of CO adsorption on surface metal sites can be effectively studied by means of infrared emission spectroscopy.

Introduction

Fourier transform infrared emission spectroscopy (FT-IRES) is rarely used in the characterization of catalysts. It has several advantages compared to the common IR absorption technique. The application of IR transmission spectroscopy is limited as the support absorbs infrared radiation below roughly 1300 cm^{-1}. This limitation is not valid for IRES. The sample is the light source itself, therefore there is no need for additional light sources in IRES. A self-supporting disk of the catalyst with certain mechanical strength is not necessary, because the sample should be accessible only from one side, so it can be placed on a horizontal sample holder. IRES is useful for studying real catalysts in the presence of adsorbates and at reasonably high catalytic temperatures, as the intensity of the signal grows with increasing sample temperatures. Highly absorbing catalysts and nontransparent black powdered samples can be effectively studied in the low-wavenumber IR region by this method. It is possible to study both surface adsorbate and solid-state support vibrations simultaneously over thin samples. IRES can be considered as an alternative to the more commonly used absorption, reflection and photoacoustic techniques.[1] Emission spectroscopy is not popular in catalytic research, because the spectra are complex: sample composition, thickness, refractive index, and geometry influence the data.[2] Besides the work of our group, few reports can be found in the literature on IRES studies, e.g., dehydroxylation of alumina gels has been followed in situ at elevated temperatures.[3,4]

Most vibrational data are available for CO adsorbed on crystal surfaces. The stretching wavenumber of CO adsorbed on metal surfaces has been the workhorse of IR reflection spectroscopy.[5] The popularity of this method can be explained partly by the convenient wavenumber range (2100−1800 cm^{-1}) and partly by the high transition dipole moment of CO stretching vibration. The assignment of terminal, 2-, 3-, or even 4-fold CO vibrations is based on the analogy to metal carbonyls where CO is bonded to a single metal atom or bridging between several metal atoms. Vibrational spectra of CO adsorbed on supported platinum metal catalysts have shown that stretching wavenumbers and relative intensities of the CO bands are sensitive to oxidation state, particle size, and metal−support interaction. These spectra have been intensively studied at room or low (liquid N_2) temperatures.[6] Only one group has characterized similar catalysts by a high-temperature transmission infrared cell[7] and our group studied CO adsorption on pure metal powders (Pd-black, Pt-black, Rh-black) by emission up to 393 K.[8,9] We identified strong CO stretching vibrations at 2043 (Pt^0−CO linear) and 1800 ($(Pt^0)_2{>}CO$ bridge) cm^{-1} for Pt/Al_2O_3, as well as symmetric and antisymmetric stretching modes of surface $Rh{<}(CO)_2$ dicarbonyl groups at 2092 and 2031 cm^{-1}, respectively, for Rh/Al_2O_3 catalysts by IRES at 420 K.[10] A weak, low-wavenumber band at 457 cm^{-1} for Pt/Al_2O_3 was attributed to the stretching vibration of Pt−C bond of linearly bonded CO, therefore we concluded that Pt−C linkages between the

---

* To whom correspondence should be addressed. Tel: +3614381100. Fax: +3614381143. E-mail: koranyi@chemres.hu.

† Chemical Research Center of the Hungarian Academy of Sciences.

‡ University of Veszprém.

10.1021/jp055745b CCC: $33.50 © 2006 American Chemical Society
Published on Web 01/12/2006

TABLE 1: Metal Content (wt %), BET Specific Surface Areas (m^2/g), Dispersion (%), and Calculated Surface Coverage, Θ (CO molecules/Surface Metal Atoms), of the Eight Catalysts at Different CO Pressures

sample	1Rh	3Rh	1Ir	3Ir	5Ir	1Pt	3Pt	5Pt
metal content[a] (wt %)	1.4	2.8	0.9	2.8	4.8	0.6	3.4	5.1
BET specific surface area[b] (m^2/g)	91	84	90	76	85	89	85	81
dispersion[c] (%)	14	9	17	14	9	14	8	4
Θ coverage at 1 Torr CO pressure ($\Theta < 1$)	0.3	0.2	0.6	0.3	0.2	1	0.4	0.5
Θ coverage at 4 Torr CO pressure ($\Theta \approx 1$)	1	0.8	3	1	0.9	5	1	2
Θ coverage at 20 Torr CO pressure ($\Theta > 1$)	5	4	13	5	4	23	7	10

[a] Determined by electron microscopy−energy dispersive X-ray analysis (EM−EDAX). [b] Determined in a dynamic system by N_2 adsorption and desorption. [c] Determined by hydrogen and oxygen titration.

adsorbate (CO) and the substrate (Pt) might be detectable by IRES, contrary to the traditional transmission technique.[10] This conclusion was recently confirmed by surface IRES under ultrahigh vacuum conditions at 200 K.[11]

The spectra of CO adsorbed on metals are similar to and well interpretable with the spectra of corresponding metal carbonyl complexes.

Our objective in this research is to extend the IRES studies in a more systematic way to higher temperatures in order to obtain information about the effect of metal dispersion and surface CO coverage on the mode of CO adsorption over alumina-supported platinum metal catalysts. Theoretical calculations of vibrations were done for three different purposes: to obtain the metal−carbon and CO stretching force constants of surface species from the experimental CO stretching vibrations; to compare the dicarbonyl, linearly bonded and bridged CO force constants of the three different metals; to estimate the Me−C≡O group deformation wavenumbers and metal−carbon stretching vibrations that are hard to measure in order to appreciate the strength of metal substrate−surface CO adsorbate bonding.

Experimental Section

Samples. Alumina-supported 1, 3, and 5 wt % Rh, Ir, and Pt metal-containing catalysts (designation: 1Rh, 3Ir, etc.) were prepared by impregnation of the alumina support with aqueous solutions of $RhCl_3$, $IrCl_3$, and $K_2Pt_2Cl_4$. After impregnation, the dried catalysts were calcined in air for 3 h at 773 K and reduced in a hydrogen stream for 4 h at 673 K. Their correct compositions, specific surface areas, and dispersions are presented in Table 1.

Instrumentation of IRES. The IRES measurements were performed on a commercial BIO-RAD (Digilab) FTS-175C Fourier Transform FT-IR spectrometer equipped with a MCT (mercury−cadmium−telluride) detector. The IR source was replaced with a homemade, electrically heated emission cell placed in focus of an off-axis ellipsoidal mirror (collector). The emission cell, which has a heated metal support and exchangeable optical windows, is suitable for in situ studies of catalysts.[1] The temperature of the sample is checked by a directly connected thermocouple and regulated by a temperature-controlled heater and cooling water. The gas volume of the cell is minimized and can be evacuated or filled through a gas inlet.

IRES Measurements. The powdered samples (∼10 mg) were pressed in the sample holder of the emission cell, then heated to 523 K under vacuum and reduced for 1 h in static hydrogen (60 kPa) at the same temperature. After evacuation, the sample was cooled in static hydrogen (60 kPa), and background IR spectra were collected at the subsequent reaction temperatures (473 and 423 K). After consecutive evacuations, 1, 4, and 20 Torr CO was adsorbed at $\Theta = 0.2-20$ CO molecules/surface metal atoms calculated surface coverages (Table 1) over the samples, first at 423 K then at 473 K, and their emission IR spectra were collected. The calculated Θ CO surface coverages can be regarded as rough estimates only, because presumably many other CO molecules are adsorbed on other cool surfaces in the emission cell and on the glassware. Generally, we claim only that the Θ coverages are below 1 at 1 Torr, around 1 at 4 Torr, and above 1 at 20 Torr CO pressures ($\Theta < 1$, $\Theta \approx 1$, and $\Theta > 1$). For comparison purposes, transmission IR spectra were also collected with the same samples at room temperature (297 K) and at 1 and 20 Torr CO pressures. (Surface Θ coverages could not be calculated for the transmission spectra, because the dead volume of the CO adsorption apparatus was high.)

CHART 1

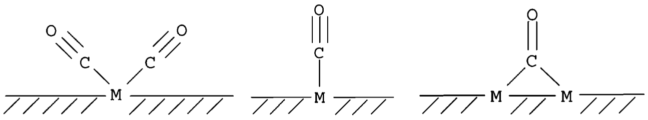

(a) dicarbonyls (C_{2v} point group) **(b)** linearly bonded CO ($C_{\infty v}$ point group) **(c)** bridged CO structures (C_{2v} point group)

Theoretical Calculations

The selected model surface species are shown in Chart 1. By analogy with metal carbonyls we have assumed the C−O equilibrium interatomic distances for the model surface species as 116, 117, and 120 pm for linear, dicarbonyl, and bridged structures, respectively. The metal−carbon bond length were estimated as 180 pm for linear species and 190 pm for all others. The $Me{<}C_2$ and $Me_2{>}C$ bond angles were assumed to be 85° both for dicarbonyls and for bridged surface species. The atomic weights of the surface metal atoms were chosen as masses in the calculations. The normal coordinate analysis and force constant calculations were carried out by a home-developed program system.[12]

Results and Discussion

The blackness of the samples is characteristic of their measurability by emission radiation. The extent of the "black-body" radiation of these samples (Figure 1) is neither connected directly with the metal loading nor with the specific surface areas but mainly with the quality of the noble metal (Pt > Rh > Ir at 473 K).

Three kinds of CO bands were identified in most of the IR spectra. The bands are well seen and best resolved in the spectra of Rh-containing catalysts (Figure 2). The broad band (∼1870 cm^{-1}) with a shoulder on the low wavenumber side is due to a bridged $(Rh^0)_2{>}CO$ species[9,13] and appears in the emission spectra only. The bands between 2000 and 2100 cm^{-1} (Figure 2) are associated with two species: a doublet is attributed to symmetric (2085−2092 cm^{-1}) and antisymmetric (2011−2022 cm^{-1}) stretch of gem-dicarbonyl $Rh^+{<}(CO)_2$ dimer vibrations and a singlet band (2049−2063 cm^{-1}) is assigned to CO linearly bonded to metallic rhodium (Table 2).[6,9,10,13,14] The geminal

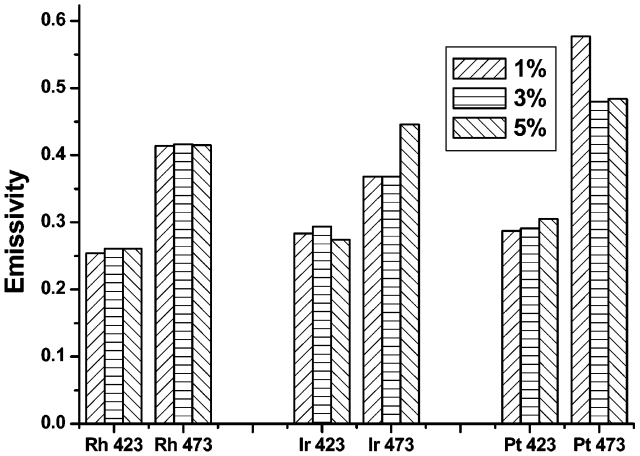

Figure 1. The relative integrated intensities of the single-beam spectra of the "blackbody" radiation of the eight catalysts at 423 and 473 K.

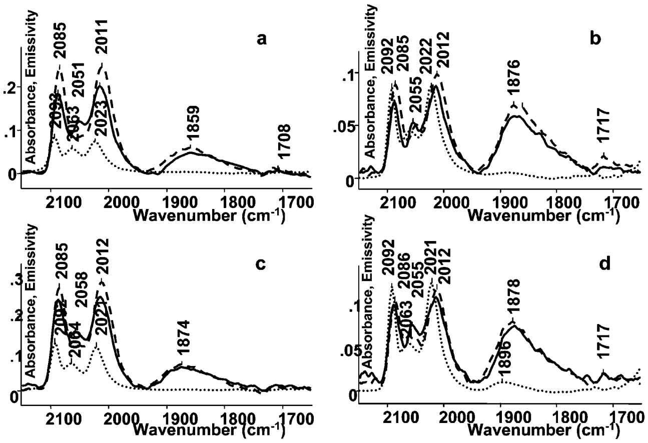

Figure 2. CO bands in the IR spectra of $1Rh/Al_2O_3$ $\Theta < 1$ (a), $3Rh/Al_2O_3$ $\Theta < 1$ (b), $1Rh/Al_2O_3$ $\Theta > 1$ (c) and $3Rh/Al_2O_3$ $\Theta > 1$ (d) catalysts at 297 K (dotted lines) 423 K (full lines) and 473 K (dashed lines).

$Rh^+<(CO)_2$ species are believed to be very stable because of their stable 18- or 16-electron configuration in the $Rh^+<(CO)_2$ surface complexes; the monocarbonyls are generally neutral.[15] The intensity of the Rh^0-CO linear band slightly decreases with increasing temperature compared to the intensities of the $Rh^+<(CO)_2$ dimer bands. The intensity of the bands of the bridged CO species compared to the signals of the dimer and linear CO vibrations increases with Rh metal loading (Figure 2) in accordance with the literature.[13] All bands above 2000 cm^{-1} are shifted toward lower wavenumbers with increasing temperatures due to the slight increase in the Rh−C bond strength.

The splitting of the $Ir^+<(CO)_2$ dicarbonyl doublet (Figure 3) is less pronounced than that of the $Rh^+<(CO)_2$ signals, which means that some intense linear Ir^0-CO stretching component is included around 2025 cm^{-1} (Table 2) in the intensity of the band in the 1900−2100-cm^{-1} region. The relative intensities of linearly bonded and bridged CO species are lower than are those in the Rh spectra. Similarly to the behavior in the case of rhodium, the linear Ir^0-CO related to $Ir^+<(CO)_2$ dimer band intensities slightly decrease with increasing temperature. The sharpness of bands in the emission spectra is much better than that in the transmission spectra (Figure 3). Erdõhelyi et al.[16] have published a similar assignment of transmission IR bands for adsorption of CO on a 5% Ir/Al_2O_3 catalyst, but in their case the stretching wavenumbers appeared at roughly 25 cm^{-1} higher positions, presumably due to higher (60%) metal dispersion of this catalyst.

The assignment of the Pt spectra (Figure 4) is the most difficult. Raskó[17] has attributed a three-band fine structure for the vibrations of CO on oxide-supported Pt catalysts observed by diffuse reflectance Fourier transform: stretching of CO on monatomic Pt^0 (2110 cm^{-1}), Pt atoms on edges (2070 cm^{-1}), and kinked Pt atoms (2050 cm^{-1}). Bourane and Bianchi[18] have found intense linearly bonded (2073−2054 cm^{-1}) and weak multibound CO species in the transmission spectra of a 3% Pt/Al_2O_3 catalyst and observed a shift of the Pt^0-CO linear band to lower wavenumbers with increasing the temperature. Stakheev et al.[19] have identified linearly bonded (2082 and 2056 cm^{-1}) and dicarbonyl (2123 and 2092 cm^{-1}) band pairs in the transmission spectra of chemisorbed CO on Pt/H−ZSM-5 zeolites. Upon thermodesorption the linearly bonded CO bands shifted toward lower wavenumbers and in parallel they could be easily removed. The dicarbonyl bands did not exhibit this coverage-dependent shift.[19]

To facilitate the assignment of bands in the Pt spectra, curve-fitting of the IR bands was performed. It gave one small, two sharp, and two broad bands in the 1900−2150-cm^{-1} spectral region (Figure 5). The sharp bands at 2084 and 2066 cm^{-1} are attributed to symmetric and antisymmetric dicarbonyl stretching vibrations, the broad bands (2034 and 2000 cm^{-1}) are assigned to linear Pt^0-CO stretchings (Table 2) based upon the results of Stakheev et al.[19] The lower wavenumbers than those reported in the literature[17−19] are attributed to the relatively low dispersion (4−14%, see in Table 1) and high emission temperature of the samples. The existence of two different linear stretchings can be explained in many different ways. The bands at higher wavenumbers can be attributed to "high coordinated", those at lower wavenumbers to "low coordinated" sites.[20] The signal at 2034 cm^{-1} can be assigned to CO adsorbed on kinked Pt atoms; the band at 2000 cm^{-1} can be attributed to CO adsorbed on platinum crystalline planes.[17] The higher intensity of symmetric (2084 cm^{-1}) compared to antisymmetric (2066 cm^{-1}) dimer stretching bands indicates that the OC−Pt−CO bond angle is less than 90°.[21]

The complex structure of the Pt−CO stretching bands is illustrated in Figure 6. The relative intensity of the right side of the band (linear Pt−CO stretching band pair) compared to the dicarbonyl vibrations decreases with increasing metal loading due to decreasing metal dispersion (Table 1). The relative intensity of linear Pt−CO bands increases with increasing temperature and also with increasing CO coverage, and the shift toward higher wavenumbers due to their coverage-dependent behavior. Dicarbonyl stretching bands do not exhibit a coverage-dependent shift. By comparison of transmission to emission spectra, the average stretching wavenumbers of dicarbonyl bands are much closer to each other than those of linear bands (Table 2), which indicates again the coverage and structure sensitivity of the latter compared to the former wavenumbers.

It is well-known that for supported metal catalysts the self-supporting pellets are usually opaque in the region below 1200 cm^{-1}. The new possibilities of using IRES instead of transmission techniques to catalytic systems have been widely discussed.[22−24] In addition to the strong CO stretching vibrations for supported Pt catalysts (supports: NaY and Al_2O_3), weak low wavenumber bands at 465 and 457 cm^{-1} were observed, which were attributed to the stretching vibrations of Pt−C bonds of linearly bonded CO.[10,25] These types of experiments are always very difficult and need special expertise. Therefore it would be of great interest to predict metal−carbon stretching

TABLE 2: Average Stretching Wavenumbers (cm^{-1}) of Examined Catalysts (Me = Rh, Ir, or Pt) at Different Surface CO Coverages

		$Me^+<(CO)_2$ dicarbonyl		Me^0-CO		$(Me^0)_2>CO$	
Me	temperature (K)	symmetric	antisymmetric	linear		bridged	
Rh	297[a]	2092	2022	2063			
Rh	423[b]	2088	2014	2053		∼1870	
Rh	473[b]	2085	2011	2049		∼1870	
Ir	297[a]	2055	∼1970	∼2025			
Ir	423[b]	2064	1993	∼2025		∼1750	
Ir	473[b]	2063	1988	∼2025		∼1750	
3Pt	297[a]	2087	2068	2044	2010	1859	1822
1Pt	423[b]	2073	2051	2003	1954	1771	1712
3Pt, 5Pt	423[b]	2085	2069	2037	1996	1847	1805
1Pt	473[b]	2066	2038	1996	1960	∼1720	
3Pt, 5Pt	473[b]	2085	2069	2039	2000	1850	1809

[a] Transmission. [b] Emission.

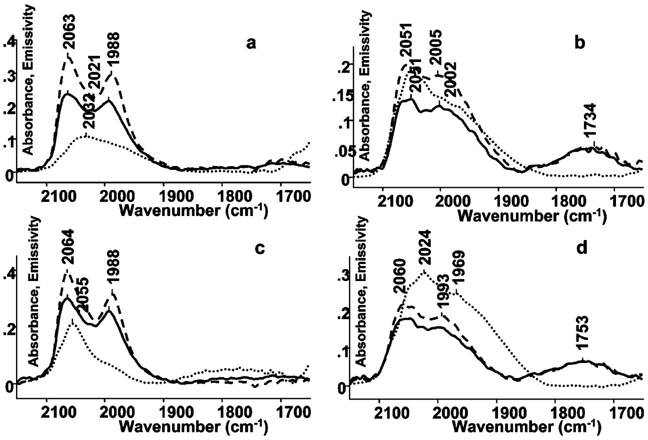

Figure 3. CO bands in the IR spectra of $1Ir/Al_2O_3$ $\Theta < 1$ (a), $3Ir/Al_2O_3$ $\Theta < 1$ (b), $1Ir/Al_2O_3$ $\Theta > 1$ (c), and $3Ir/Al_2O_3$ $\Theta > 1$ (d) catalysts at 297 K (dotted lines), 423 K (full lines), and 473 K (dashed lines).

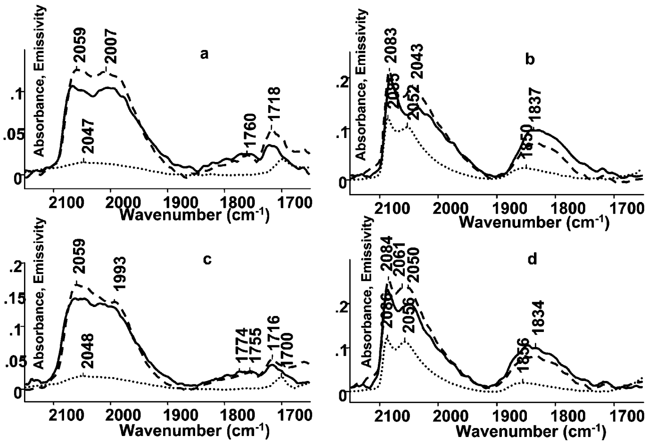

Figure 4. CO bands in the IR spectra of $1Pt/Al_2O_3$ $\Theta < 1$ (a), $3Pt/Al_2O_3$ $\Theta < 1$ (b), $1Pt/Al_2O_3$ $\Theta > 1$ (c), and $3Pt/Al_2O_3$ $\Theta > 1$ (d) catalysts at 297 K (dotted lines), 423 K (full lines), and 473 K (dashed lines).

modes on the basis of CO stretching vibrations without tedious and difficult experimental efforts.

It can be assumed that the CO stretching force constants calculated on the basis of selected surface species (Chart 1) are more realistic than those obtained by the widely used diatomic approximations. The potential energy distributions of the model surface species have shown that the contributions of metal-stretching vibrations to the normal modes in question are around 5−10%. On the basis of CO force constants obtained for different surface species, the metal−carbon vibrations can be predicted using the following correlations.

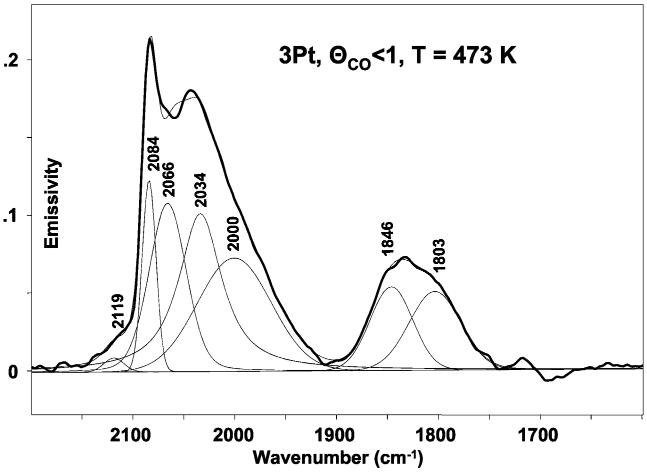

Figure 5. Curve-fitting of CO bands in the IR spectrum of $3Pt/Al_2O_3$ catalyst at $\Theta < 1$ CO coverage and $T = 453$ K emission temperature.

Cotton[26] has given an approximate empirical expression for the determination of CO bond order (n(CO)) based on CO stretching force constant (K(CO) in $N\cdot cm^{-1}$)

$$n(CO) = 0.155K(CO) + 0.124 \qquad (1)$$

If one considers that the total bond order of the carbon atom is 4, the bond order of metal−carbon bond (n(Me−C)) can be easily calculated. The metal−carbon force constant (K(Me−C) in $N\cdot cm^{-1}$) can be obtained by eq 2

$$K(Me-C) = An(Me-C) \qquad (2)$$

where A is different for different metals; it is generally 3.13, 2.70, and 2.53 for Ir, Rh, and Pt species, respectively. The value of parameter A can be obtained from the results of normal coordinate calculations of metal carbonyls.

The dominant surface species are the $Me<(CO)_2$ dicarbonyl formations on the Rh and Ir catalysts, while the Pt−CO linear species on Pt surfaces are prevailing under our experimental conditions. The *cis*-$[MeX_2(CO)_2]^{n-}$ (Me = Pt^{2+}, Rh^+, Ir^+, and X = Cl^-, Br^-) organometallic complexes[27] provide an excellent vibrational spectroscopic analogy to identify $Me<(CO)_2$ type dicarbonyl surface species despite their different charges and metallic oxidation states. Their selected stretching vibrational wavenumbers are shown in Table 3.

The separation of symmetric and antisymmetric stretchings is 63−85 cm^{-1} both in the complexes and surface dicarbonyls

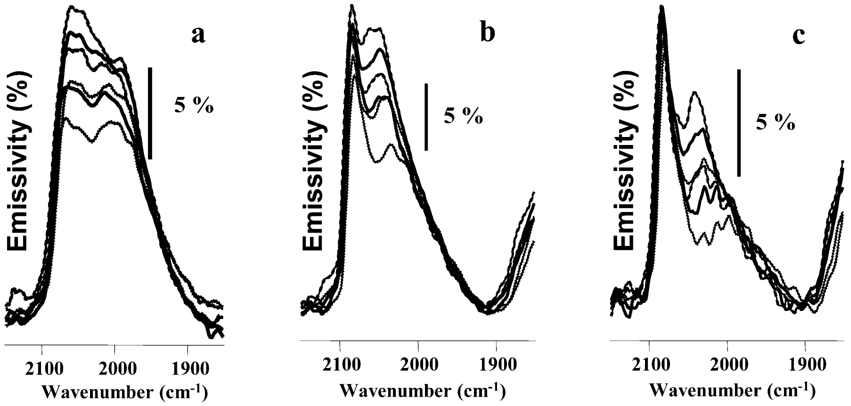

Figure 6. Pt−CO stretching bands of $1Pt/Al_2O_3$ (a), $3Pt/Al_2O_3$ (b), and $5Pt/Al_2O_3$ (c) catalysts at $\Theta < 1$ (dotted lines), $\Theta \approx 1$ (full lines), and $\Theta > 1$ (interrupted lines) CO coverages at 423 and 473 K emission temperatures.

TABLE 3: Comparison of Experimental Fundamental Stretching Wavenumbers (ν in cm^{-1}) of Anionic $[MeCl_x(CO)_y]^-$ Complexes and $Me_x(CO)_y$ Surface Species as Well as Calculated Metal−Carbon Stretching Modes (in parentheses) and Force Constants (K = valence, k = valence−valence in $N{\cdot}cm^{-1}$) of Surface CO Groups[a]

	CO	symmetric		antisymmetric		force constants ($N{\cdot}cm^{-1}$)			
Me	mode	a_1 ν(CO)	ν(Me-C)	b_1 ν(CO)	ν(Me-C)	K(CO)	K(Me-C)	k(CO, CO)	k(MeC, MeC)
$[RhCl_2(CO)_2]^-$[27]	dicarbonyl	2070	492	1992	455	15.43	3.21	0.61	0.30
$Rh<(CO)_2$	dicarbonyl	2092	(470)	2022	(432)	16.17	2.73	0.53	0.15
$[IrCl_2(CO)_2]^-$[27]	dicarbonyl	2056	548	1973	526	14.81	4.51	0.68	0.02
$Ir<(CO)_2$	dicarbonyl	2055	(528)	1970	(506)	14.89	4.22	0.65	0.12
$[PtCl_2(CO)_2]$[27]	dicarbonyl	2175	460	2134	430	17.63	3.06	0.24	0.22
$Pt<(CO)_2$	dicarbonyl	2086	(462)	2069	(440)	16.38	3.11	0.10	0.11
$Rh(CN)(PPh_3)_2(CO)$[28]	linear	2003	486			15.86	3.83		
Rh−CO	linear	2055	(474)			16.00	3.10		
$Ir(CN)(PPh_3)_2(CO)$[28]	linear	1990	526			15.66	4.53		
Ir−CO	linear	2025	(512)			15.12	4.14		
$[PtCl_3(CO)]^-$[29]	linear	2097	497			16.47	3.91		
Pt−CO	linear	2040	(475)			15.61	3.51		
		2005	(494)			14.91	3.84		
		1994	(498)			14.70	3.91		
		1958	(512)			14.01	4.18		
$[Pd_2Cl_4(CO)_2]^{2-}$[30]	bridged	1937[b]	446[b,c]		405[b,c]				
$Rh_2>CO$	bridged	1870	(538)[c]		(498)[c]	12.61	3.17		0.88
$Ir_2>CO$	bridged	1750	(560)[c]		(520)[c]	10.36	3.89		1.35
$Pt_2>CO$	bridged	1855	(481)[c]		(441)[c]	12.60	2.82		0.83
		1803	(540)[c]		(500)[c]	11.36	3.58		1.17

[a] Additional results, e.g., Me−CO linear bendings, angle bending wavenumbers, and force constants are available on request. [b] Mean of IR and Raman wavenumbers. [c] $Me_2>C$ stretching.

in the case of Rh and Ir. Contrary to this, the same separation is 41 cm^{-1} only in the Pt complex[27] and even smaller (17 cm^{-1}) in the $Pt<(CO)_2$ surface species (Table 3).

The strength (force constant) of CO bonds changes in the Pt > Rh > Ir order for dicarbonyl surface species similar to those for the $[MeCl_2(CO)_2]^-$ organometallic complexes (Table 3). Generally the strength of metal−carbon bonds changes in the opposite direction than the CO force constants, which is valid in the metal complexes (Table 3). The Me−C bond strength order is Ir ≫ Pt > Rh in the surface dicarbonyls; that is, Pt precedes Rh. In the case of $Ir<(CO)_2$ the weak CO and strong Ir−C bond points to the fact that both the CO donation and the Ir back-donation ability is the strongest among the three metals. The small CO force constant difference between Pt and Rh seems to confirm that the back coordination on the Pt surface is enhanced compared to the Rh surface. Clearly the 4d orbitals are less available for π-donation to CO in the rhodium systems than for the corresponding iridium and platinum systems.

The linearly bonded CO species can be classified to the $C_{\infty v}$ point group, and as they are oriented perpendicularly to the surface, only the CO and MeC stretching vibrations will be active in the infrared spectrum due to the surface selection rules.

It was difficult to find monocarbonyl Rh and Ir complexes with full experimental and calculated data. The *trans*-$Me(CN)(PPh_3)_2(CO)$ (Me = Rh^+, Ir^+) complexes[28] were used finally to compare the CO stretching wavenumbers. For Pt−CO linear species, the $[PtCl_3(CO)]^-$ complex[29] was used as a comparison. Similar to surface dicarbonyls in linear Me−CO species, the Ir−C bond is the strongest, which is followed by the Pt−C bond, and the weakest is the Rh−C bond. The order of CO stretching *wavenumbers* is just the opposite: Rh > Pt > Ir (2055 > 2040 > 2025 cm^{-1}), which clearly reflects the decreasing trends of the CO stretching force constants: 16.00 > 15.61 > 15.12 $N{\cdot}cm^{-1}$, respectively. The metal−carbon stretching force constants increased by 15−40% for Pt and Rh linear complexes and surface species, as compared to those of dicarbonyls, while the Ir−C force constants showed minimal changes (Table 3).

As it was tabulated in Table 2, several bridging $Me_2>CO$ bands were observed in the 1720−1870-cm^{-1} wavenumber region. Ir and Rh catalysts exhibited bridging CO species only at higher temperatures (423 and 473 K). Pt showed stronger and more complicated spectral features in this region at any temperatures. Bands were observed around 1771 and 1712 cm^{-1} at low (1%) Pt content (at high dispersion), while at higher (3

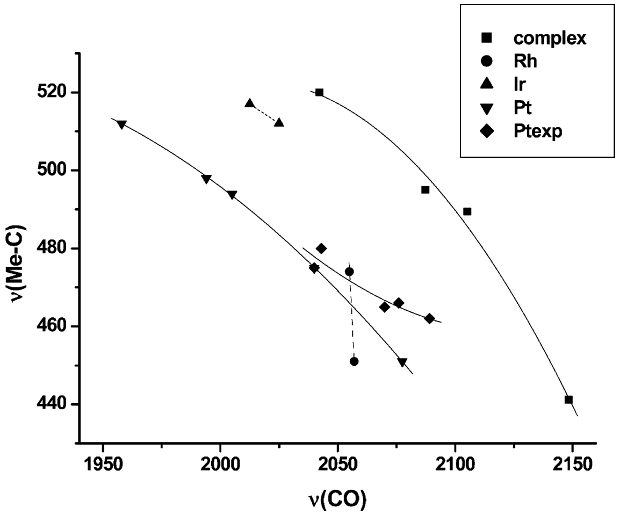

Figure 7. Relationship between Me−C and CO stretching wavenumbers (ν) for platinum carbonyl complexes, Rh-, Ir-, and Pt surface species. Experimental values of Pt surface species (Pt exp) are gained from the literature.[25,31]

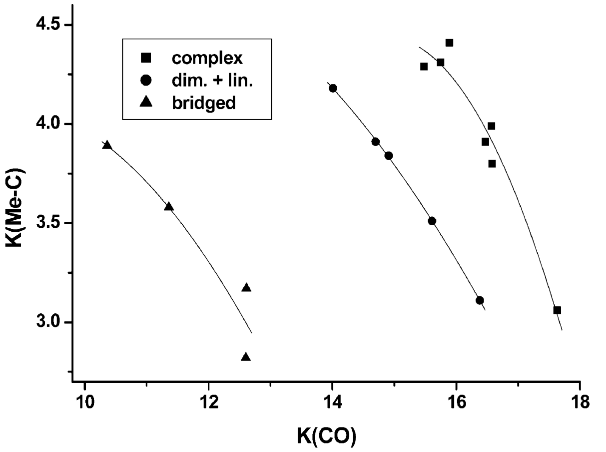

Figure 8. Relationship between Me−C and CO force constants (K) for platinum complexes, dimer + linear Pt, and bridged Rh, Ir, and Pt surface species.

and 5%) metal contents another two bands were recorded around 1855 and 1803 cm^{-1} (averaged values) (Figures 4 and 5). Force constant calculations were performed for the bridging CO species as well, but to obtain spectroscopic data for noble metal carbonyls with a bridging CO group was not an easy task. Therefore we tried to compare vibrations of the dimeric $[Pd_2Cl_4(CO)_2]^{2-}$ complex[30] with CO bridges (Table 3). The lower CO stretching band of $Ir_2{>}CO$ species lead to the strongest metal−carbon stretching force constants (3.89 N·cm^{-1}), which agrees with the highest wavenumber pairs (560/520 cm^{-1}) for symmetric and antisymmetric $Ir_2{>}C$ stretchings, respectively. The CO force constant of $Ir_2{>}CO$ (10.36 N·cm^{-1}) gives the CO bond order by eq 1 lower than two (1.73), while it is higher than two (2.08) for bridged carbonyls on Rh and on Pt. It means that the bridging CO groups on iridium form very strong Ir−C bonds due to the strong back-donation of 5d orbitals to CO.

According to the previous discussions, some correlation should exist between the CO and Me−C wavenumbers and force constants. The relationship between CO and Me−C stretching wavenumbers for platinum carbonyl complexes[29] and for linearly bonded and dicarbonyl surface species (Table 3) was plotted in Figure 7. The donor capabilities of different ligands and different metal charges are scattered the Me−C stretching wavenumbers of platinum carbonyl complexes between 440 and 520 cm^{-1}. The curve of platinum surface species exhibits a plotting similar to the graph of the complexes, but the former is shifted with 60−80 cm^{-1} to lower wavenumbers. The dicarbonyl and linearly bonded rhodium surface species and other experimentally available adsorbed Pt−CO wavenumber data[25,31] also fit the curve of platinum surface species, but the wavenumbers of surface iridium species are between the two graphs. These correlations can also be used to predict metal−carbon stretching wavenumbers for chemisorbed CO species.

The relationship between CO and Me−C stretching force constants is presented in Figure 8. The general pattern of curves obtained for the wavenumbers (Figure 7) and force constants (Figure 8) of Pt−carbonyl complexes and platinum surface species is very similar. The data points are scattered in case of force constants of the complexes, which is due to the fact that the Pt−C stretching mode is strongly coupled with other vibrations of the complex and the Pt−C force constants are sensitive to coordination sphere, oxidation state, and overall charge of platinum. The lowest Pt−C force constants were observed in both cases for dicarbonyls, 3.06 N·cm^{-1} for $PtCl_2(CO)_2$ and 3.11 N·cm^{-1} for $Pt{<}(CO)_2$ surface formation (Table 3). In dicarbonyls the two CO ligands have to share the back-donation from the d orbital of platinum; consequently the Pt−C bond is weakened. The curves of platinum surface species and complexes are similar (both in Figures 7 and 8), but the surface species have more than 1.0 N·cm^{-1} lower CO force constants (Figure 8). Since the CO bond order in the bridged species is nearly 2 (Chart 1c), the CO stretching force constants are also drastically lowered to 10.4−12.6 N·cm^{-1} (Table 3). Both metal atoms are donating electrons to the same CO in a competitive way in bridged carbonyls; consequently the individual metal−carbon bonds are weakened. On the other side, the two metal−carbon bonds together can bind the bridged CO very strongly, therefore the stability (strength of adsorption) is very high for bridged species.

The running of curves shown in Figures 7 and 8 exhibits a general trend according to which the CO and metal−carbon bonds are always stronger in metal carbonyl complexes than in adsorbed surface species.

Conclusions

The peak positions in the transmission (297 K) and emission (423 and 473 K) spectra are close to each other, but the relative intensities and sharpness of bands in the emission spectra show a more detailed spectral structure. Presumably, the surface CO coverage is lower in the samples studied by emission than those examined by transmission, because the relative intensity of bridged CO bands around 1800 cm^{-1} is higher in the emission than in the transmission spectra. CO adsorbs in dicarbonyl, linearly bonded, and bridged forms on every catalyst at both emission temperatures; the three forms are best resolved on rhodium; the band structure is the most complex on platinum. The surface structure of the catalyst and the distribution of $Me_x(CO)_y$ (Me = metal) surface adsorbed species can be finely tuned by the temperature and the surface CO coverage.

The vibrational spectra of surface species showed reasonable similarities with the spectra of selected metal carbonyl complexes. Force constant calculations were performed for the three (dicarbonyl (dimer), linearly bonded (on-top) CO, and bridging carbonyl) model surface formations. The CO stretching force constants were fitted to the experimentally observed wavenumbers and with a special approximation the metal−carbon stretching wavenumbers and force constants were predicted. The iridium−carbon bonds were found always stronger than the

Rh−C and Pt−C ones in all surface species. The stability of different surface species can be judged using the metal−carbon stretching force constants. The metal substrate−surface CO adsorbate bonding strength correlates with the metal−carbon bonding force constant in the corresponding metal carbonyl complexes. The observed stretching wavenumbers and force constants seem to support the idea that CO and metal−carbon bonds are always stronger in metal carbonyl complexes than in adsorbed surface species.

Acknowledgment. This work was supported in part by The Hungarian Science Foundation (OTKA Grant No. T-35115). Special thanks are due to Prof. J. Petró for preparation of the catalysts.

References and Notes

(1) Mink, J. In *Handbook of Vibrational Spectroscopy*; Chalmers, J. M., Griffiths, P. R., Eds.; Wiley: New York, 2002; Vol. 2, p 1193.

(2) Ryczkowski, J. *Catal. Today* **2001**, *68*, 263.

(3) Frost, R. L.; Kloprogge, J. T.; Russell, S. C.; Szetu, J. L. *Thermochim. Acta* **1999**, *329*, 47.

(4) Kloprogge, J. T.; Frost, R. L. *Appl. Catal. A* **1999**, *184*, 61.

(5) Pritchard, J. *J. Vac. Sci. Technol.* **1972**, *9*, 895.

(6) Hadjiivanov, K. I.; Vayssilov, G. N. *Adv. Catal.* **2002**, *47*, 307.

(7) Chafik, T.; Dulaurent, O.; Gass, J. L.; Bianchi, D. *J. Catal.* **1998**, *179*, 503.

(8) Mink, J.; Keresztury, G.; Szilágyi, T.; Tétényi, P. *J. Mol. Struct.* **1993**, *293*, 283.

(9) Bódis, J.; Németh, Cs.; Mink, J.; Keresztury, G.; Tétényi, P. *J. Mol. Struct.* **1997**, *410−411*, 179.

(10) Mink, J.; Szilágyi, T.; Wachholz, S.; Kunath, D. *J. Mol. Struct.* **1986**, *141*, 389.

(11) Scholes, F. H.; Locatelli, A.; Kleine, H.; Ostanin, V. P.; King, D. A. *Surf. Sci.* **2002**, *502−503*, 249.

(12) Mink, J.; Mink, L. Computer Program System for Vibrational Analysis of Polyatomic Molecules. In *Lahey-Fujitsu Fortran Win32*; Stockholm, 2004.

(13) Dulaurent, O.; Chandes, K.; Bouly, C.; Bianchi, D. *J. Catal.* **2000**, *192*, 262.

(14) Frank, M.; Kühnemuth, R.; Bäumer, M.; Freund, H.-J. *Surf. Sci.* **2000**, *454−456*, 968.

(15) Hadjiivanov, K.; Ivanova, E.; Dimitrov, L.; Knözinger, H. *J. Mol. Struct*. **2003**, *661−662*, 459.

(16) Erdõhelyi, A.; Fodor, K.; Suru, G. *Appl. Catal. A* **1996**, *139*, 131.

(17) Raskó, J. *J. Catal.* **2003**, *217*, 478.

(18) Bourane, A.; Bianchi, D. *J. Catal.* **2003**, *218*, 447.

(19) Stakheev, A. Yu.; Shpiro, E. S.; Tkachenko, O. P.; Jaeger, N. I.; Schulz-Ekloff, G. *J. Catal.* **1997**, *169*, 382.

(20) Tolenaar, F. J. C. M.; Bastein, A. G. T. M.; Ponec, V. *J. Catal.* **1983**, *82*, 35.

(21) Braterman, P. S. *Metal Carbonyl Spectra*; Academic Press: London, 1975.

(22) Mink, J. *Mikrochim. Acta* **1987**, *3*, 63.

(23) van Woerkom, P. C. M. FTIR Studies of Catalyst Systems under Realistic Processing Conditions. In *Advances in Applied Fourier Transform Infrared Spectroscopy*; Mackenzie, M. W., Ed.; Wiley: Chichester, 1988; pp 323−347.

(24) Mink, J.; Keresztury, G. *Appl. Spectrosc.* **1993**, *47*, 1446.

(25) Primet, M.; Foulloux, P.; Imelik, B. *J. Catal.* **1980**, *61*, 553.

(26) Cotton, F. A. *Inorg. Chem.* **1964**, *3*, 702.

(27) Goggin, P. L.; Mink, J. *Inorg. Chim. Acta* **1979**, *34*, 225.

(28) Vaska, L.; Pene, *J. Chem. Commun.* **1971**, 418.

(29) Mink, J.; Goggin, P. L. *Can. J. Chem.* **1991**, *69*, 1857.

(30) Goggin, P. L.; Mink, J. *J. Chem. Soc. (Dalton)* **1974**, 534.

(31) Tobin, R. G.; Richards, P. L. *Surf. Sci.* **1987**, *179*, 387.